

# ChemComm

Accepted Manuscript



This article can be cited before page numbers have been issued, to do this please use: C. Zhang, S. Wang and B. Tan, *Chem. Commun.*, 2017, DOI: 10.1039/C7CC06702J.



This is an Accepted Manuscript, which has been through the Royal Society of Chemistry peer review process and has been accepted for publication.

Accepted Manuscripts are published online shortly after acceptance, before technical editing, formatting and proof reading. Using this free service, authors can make their results available to the community, in citable form, before we publish the edited article. We will replace this Accepted Manuscript with the edited and formatted Advance Article as soon as it is available.

You can find more information about Accepted Manuscripts in the [author guidelines](#).

Please note that technical editing may introduce minor changes to the text and/or graphics, which may alter content. The journal's standard [Terms & Conditions](#) and the ethical guidelines, outlined in our [author and reviewer resource centre](#), still apply. In no event shall the Royal Society of Chemistry be held responsible for any errors or omissions in this Accepted Manuscript or any consequences arising from the use of any information it contains.

Journal Name

COMMUNICATION

## Novel fullerene-based porous materials constructed by solvent knitting strategy†

Chengxin Zhang,<sup>ab</sup> Shaolei Wang<sup>ab</sup> and Bien Tan<sup>\*ab</sup>Received 00th January 20xx,  
Accepted 00th January 20xx

DOI: 10.1039/x0xx00000x

www.rsc.org/

**Here we choose a dihydronaphthyl-functionalized C<sub>60</sub> fullerene as building block and utilize a novel solvent knitting strategy based on Friedel-Crafts alkylation reaction to construct two kinds of novel porous materials by using dichloromethane(DCM) and 1,2-dichloroethane(DCE) as solvents and external crosslinkers. The resulting porous materials show relatively high apparent BET surface areas and gas uptake abilities.**

Microporous organic polymers (MOPs) have attracted wide attentions in many fields like gas storage and separation,<sup>1-3</sup> catalysis,<sup>4,5</sup> chemical sensing,<sup>6</sup> energy storage and conversion,<sup>7</sup> etc. Compared with traditional inorganic porous materials, such as zeolites and activated carbon, MOPs which consist purely of organic components have many advantages such as low skeletal density, abundant pore structure and easier functionalization,<sup>8,9</sup> which further expands the scope of applications of MOPs. Until now, many different kinds of MOPs, which were classified by the structure and synthetic strategy, have been reported, such as conjugated microporous polymers (CMPs),<sup>10,11</sup> polymers of intrinsic microporosity (PIMs),<sup>12</sup> covalent organic frameworks(COFs),<sup>13,14</sup> hyper-crosslinked polymers (HCPs),<sup>15,16</sup> porous aromatic frameworks (PAFs).<sup>17</sup> With a variety of synthetic strategies and synthetic routes, a large number of molecules with special functions can be synthesized and designed as building blocks to construct novel porous materials with various specific functions and applications.<sup>9,18</sup>

As a novel kind of three-dimensional aromatic compound with unique cage structure, fullerene, which was first reported by Kroto *et al.*,<sup>19</sup> shows a variety of applications in many fields including those in solar cells,<sup>20</sup> semiconducting materials,<sup>21</sup> electrochemical systems,<sup>22</sup> catalysis,<sup>23</sup> and biological medicine,<sup>24</sup> and have thus attracted

increased worldwide attention. Considering these unique properties and potential applications, many reports about C<sub>60</sub> and its derivatives have been published on fullerene-functionalized materials.<sup>25</sup> Recently, some porous polymers have been reported in combination with fullerenes, which are usually synthesized by two strategies: introducing fullerene into the porous frameworks by post functionalization, or focused on building fullerene-derivatives based porous materials. For example, Jiang *et al.* reported a novel electron donor-acceptor COFs, of which 2D-skeletons were built from electron-donating monomers and introduced the typical electron acceptor, fullerene, within the open channels of frameworks *via* Click chemistry.<sup>26</sup> In 2016, Zhu *et al.* firstly reported a series of C<sub>60</sub>-based PAFs materials combining both symmetrical conjugated structure of C<sub>60</sub> and the porous properties of PAFs using external crosslinker knitting method, which showed relatively high surface area of 1094 m<sup>2</sup>g<sup>-1</sup> and a comparable adsorption capacity for H<sub>2</sub> and CO<sub>2</sub>.<sup>27</sup>

It is well established that the pure fullerene C<sub>60</sub> powder only possess a certain solubility in several aromaticity solvents like toluene, but its derivatives show decent solubility in common solvents like DCM and DCE. Chemical functionalization of the fullerene cage has easily been achieved to make fullerene derivatives and promote their involvement in organic reactions. Recently, our group developed a novel solvent knitting strategy employing AlCl<sub>3</sub> as Lewis acid catalyst, chloralkane as solvents and external crosslinkers to knit HCPs materials.<sup>28,29</sup> This simple, versatile and flexible method is very useful for “knitting” aromatic compounds to construct HCPs materials with abundant porosity and without any other additional effects on the structure of building block compounds.

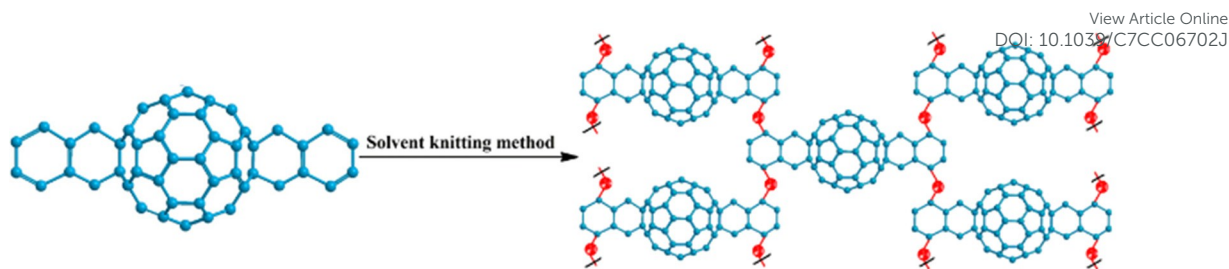
Herein, we employed a dihydronaphthyl-functionalized fullerene NC<sub>60</sub>BA (N for abbreviation)<sup>30</sup>, with excellent solubility, as the building block to construct microporous C<sub>60</sub>-based polymers which are named N-H-1 and N-H-2 by using DCM and DCE as solvent and external crosslinking agent, respectively. The resulting porous materials show high surface area, favourable gas adsorption capacity and thermal stability, and they have been thoroughly characterized to understand their structure and properties.

Although fullerenes have attracted much more attention due to vari-

<sup>a</sup> School of Chemistry and Chemical Engineering, Huazhong University of Science and Technology, Wuhan, 430074, China. E-mail: bien.tan@mail.hust.edu.cn; Tel: +86 2787558172

<sup>b</sup> Key Laboratory for Large-Format Battery Materials and System, Ministry of Education, School of Chemistry and Chemical Engineering, Huazhong University of Science and Technology, Luoyu Road No. 1037, Wuhan, 430074, China

†Electronic supplementary information (ESI) available: NMR, CP/MAS NMR, TGA, FSEM, HRTEM and isosteric heat of materials. See DOI: 10.1039/x0xx00000x



**Scheme 1.** The synthetic routes of the polymer networks (Red dots represent  $-\text{CH}_2-$  or  $-\text{CH}_2\text{-CH}_2-$ )

ous applications, but, until now, there is not much focus on the synthesis of  $\text{C}_{60}$  fullerene-based porous materials and their potential applications. As shown in Scheme 1, we have prepared two novel  $\text{C}_{60}$  based porous materials using monomer N as building block by a simple *Friedel-Crafts* reaction with two different external crosslinkers (Experimental details, ESI†). At the end of reaction, the solid insoluble products were obtained which were precipitated. In order to determine the structural features of the polymers, FT-IR and solid state  $^{13}\text{C}$  CP/MAS NMR were used for chemical characterization. The C-H stretching vibration bands of methylene linkage ( $\nu$   $-\text{CH}_2-$ ) near  $2960\text{--}2800\text{ cm}^{-1}$  are evidently observed. Compared with monomer N, the weak signals of C-H stretching vibrations of the aromatic ring ( $\nu$  Ar-H) at  $3100\text{--}3000\text{ cm}^{-1}$  disappeared after the crosslinking reactions for N-H-1 and N-H-2, as shown in Fig. 1. The intensity of out-of-plane bending vibration peaks ( $\gamma$  Ar-H) at  $910\text{--}665\text{ cm}^{-1}$  also reduced (Fig. 1(b)) or even nearly vanished (Fig. 1(c)), which suggests that most of the hydrogen atoms in benzene rings have been replaced by methylene groups. The peak near  $1425\text{ cm}^{-1}$  clearly shows the original structure of fullerene is completely preserved.<sup>27</sup> We further investigated the chemical structure of the resulting materials by  $^{13}\text{C}$  CP/MAS NMR spectra (Fig. S3, ESI†). Two peaks are clearly observed near 140 ppm and 130 ppm for monomer, which are attributed to the substituted aromatic carbons and unsubstituted aromatic carbons in the benzene rings respectively,<sup>28</sup> and a narrow peak around 60 ppm belongs to the  $sp^3$  fullerene carbons for monomer

(Fig. S3, ESI†).<sup>31,32</sup> Compared with monomer, the intensity of substituted aromatic carbon (140 ppm) and alkyl carbon peaks (40 ppm) of HCPs increased, which was ascribed to much more alkyl linkers connected with monomer (Fig. S3 (b) (c), ESI†).<sup>33</sup> These data confirmed that the solvent knitting strategy has been successfully employed for the construction of the HCPs materials.

The thermal stability of monomer N, N-H-1 and N-H-2 was recorded by thermogravimetric analysis (TGA). As shown in Fig. S4 (ESI†), the weight of N-H-1 and monomer N lost slowly and continuously, and there was no significant loss of weight until  $400\text{ }^\circ\text{C}$  for N-H-2, which may be due to the difference in their chemical nature. Moreover, the introduction of alkyl leads to lower residual variability for N-H-1 and N-H-2.

The morphologies and porous textures of the two networks were investigated by field-emission scanning electron microscopy (FE-SEM) and high-resolution transmission electron microscopy (HR-TEM) (Fig. S5, ESI†). The FE-SEM images revealed that the N-H-1 and N-H-2 showed an amorphous morphologies, and their structures are very similar. The HR-TEM images showed that there were abundant pore structure in both N-H-1 and N-H-2, which could be

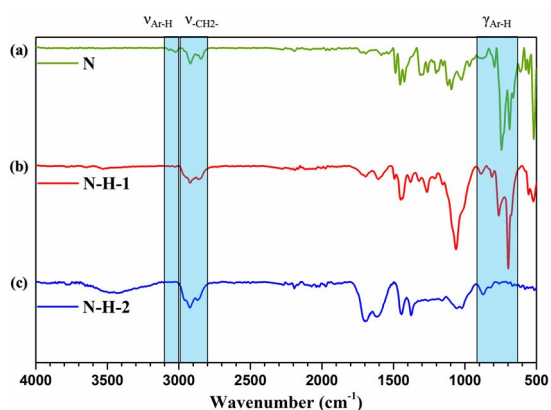


**Fig. 1** The Fourier transform infrared (FT-IR) spectra of monomer N (a), N-H-1(b) and N-H-2(c).

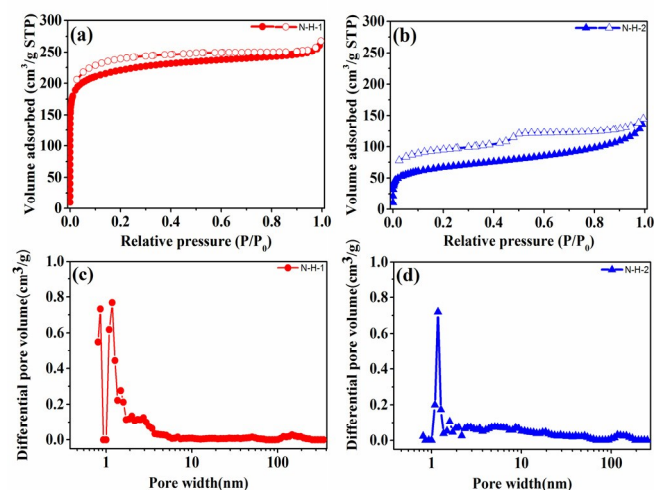


**Fig. 2** (a) (b) Nitrogen adsorption and desorption isotherms (77.3 K) and (c) (d) pore size distribution calculated using DFT methods (slit pore models, differential pore volumes) of N-H-1 (red) and N-H-2 (blue).

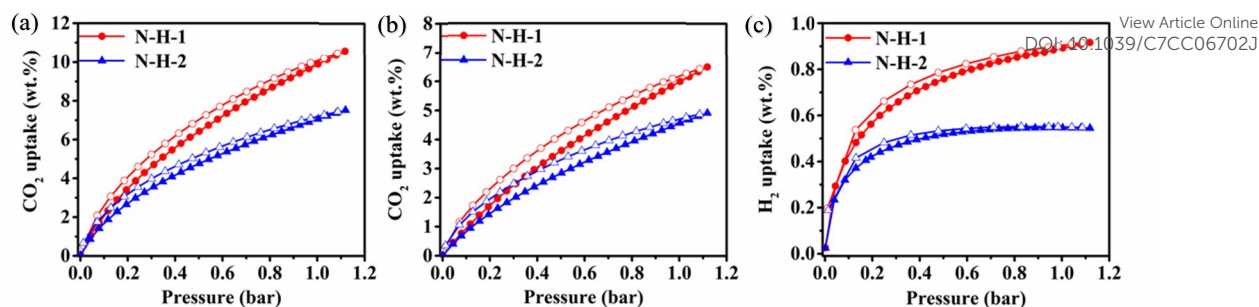


**Fig. 3** The Volumetric CO<sub>2</sub> adsorption and desorption isotherms up to 1.13 bar at 273.15 K (a), 298.15 K (b) and volumetric H<sub>2</sub> adsorption isotherms and desorption isotherms up to 1.13 bar at 77.3 K (c) of N-H-1 and N-H-2.

**Table 1** Porosity properties and gas uptake capacities of N-H-1 and N-H-2

No.	S <sub>BET</sub> <sup>[a]</sup> (m <sup>2</sup> g <sup>-1</sup> )	S <sub>L</sub> <sup>[b]</sup> (m <sup>2</sup> g <sup>-1</sup> )	PV <sup>[c]</sup> (cm <sup>3</sup> g <sup>-1</sup> )	MPV <sup>[d]</sup> (cm <sup>3</sup> g <sup>-1</sup> )	H <sub>2</sub> uptake <sup>[e]</sup> (wt %)	CO <sub>2</sub> uptake <sup>[f]</sup> (wt %)	CO <sub>2</sub> uptake <sup>[g]</sup> (wt %)
N-H-1	753	997	0.41	0.25	0.92	10.59	6.50
N-H-2	235	317	0.22	0.05	0.55	7.51	4.91

<sup>[a]</sup> Surface area calculated from nitrogen adsorption isotherm at 77.3 K using BET equation. <sup>[b]</sup> Surface area calculated from nitrogen adsorption isotherm at 77.3 K using Langmuir equation. <sup>[c]</sup> Pore volume calculated from nitrogen isotherm at P/P<sub>0</sub>=0.995, 77.3 K. <sup>[d]</sup> Micropore volume calculated from the nitrogen isotherm at P/P<sub>0</sub>=0.050. <sup>[e]</sup> H<sub>2</sub> uptake determined volumetrically using a Micromeritics ASAP 2020 M analyzer at 1.13 bar and 77.3 K. <sup>[f]</sup> CO<sub>2</sub> uptake determined volumetrically using a Micromeritics ASAP 2020 M analyzer at 1.13 bar and 273.15 K. <sup>[g]</sup> CO<sub>2</sub> uptake determined volumetrically using a Micromeritics ASAP 2020 M analyzer at 1.13 bar and 298.15K.

observed clearly.

To better understand the pore characteristics, the porous nature of polymers was further investigated by N<sub>2</sub> sorption analysis at 77.3 K. As shown in Fig.S6, the BET surface of monomer N was nearly 0 m<sup>2</sup>g<sup>-1</sup>, and there were almost no existence of micropores and mesopores (Fig.S6, ESI<sup>†</sup>). However, the adsorption isotherms of N-H-1 and N-H-2 exhibit a type I character with a high nitrogen gas uptake at low relative pressure (P/P<sub>0</sub> < 0.001), thus indicating the abundant microporous structure,<sup>34,35</sup> which are consistent with HR-TEM results. Moreover, the nitrogen adsorption and desorption isotherms provide a strong evidence that the solvent knitting methods have been successful to construct porous structures.

The BET surface area of N-H-1 and N-H-2 is up to 753 m<sup>2</sup>g<sup>-1</sup> and 235 m<sup>2</sup>g<sup>-1</sup> respectively. The pore size distribution of N-H-1 showed hierarchical pores, in which the abundant micropores (0.8 nm) and continuous mesopores (less than 10 nm) are observed clearly. From Table 1, the total pore volumes of N-H-1 and N-H-2 are 0.41 cm<sup>3</sup>g<sup>-1</sup> and 0.22 cm<sup>3</sup>g<sup>-1</sup>, respectively. It is obvious that the microporosity of N-H-1 (61%) is much higher than that of N-H-2 (23%), which may be due to the difference in the length of carbon chain (from DCM and DCE). DCM with shorter carbon chain, made the monomers connected closely and formed a much more stable and tightly packed dense structure. The compact linking structure helps in constructing micropores and increasing the surface area and pore volume. Based on the above analysis, the solvent knitting method using DCM and DCE as the external crosslinker can effectively link monomer N to obtain fullerene-based porous materials. Abundant porous structure make such porous materials excellent gas absorbents for CO<sub>2</sub> and H<sub>2</sub>, and

therefore, we also set out to investigate CO<sub>2</sub> and H<sub>2</sub> absorptive capacities of N-H-1 and N-H-2. As shown in Fig. 3a, the CO<sub>2</sub> isotherms of N-H-1 and N-H-2 are fairly consistent. Table 1 shows the values of CO<sub>2</sub> capture at different temperatures. The CO<sub>2</sub> uptake of N-H-1 and N-H-2 was found to be 10.59 wt% (2.41 mmol g<sup>-1</sup>) and 7.51 wt% (1.48 mmol g<sup>-1</sup>) at 273 K and 1.13 bar, respectively, which is comparable to that of CTF-FUMs and CTF-DCNs (2.12-3.49 mmol g<sup>-1</sup>),<sup>36</sup> Cu(II)- and Ni(II)-PCPs (2.49-2.80 mmol g<sup>-1</sup>),<sup>37</sup> HPPs (1.15-1.69 mmol g<sup>-1</sup>),<sup>38</sup> POPSS (1.84-2.21 mmol g<sup>-1</sup>),<sup>39</sup> SHCPs (1.23-1.84 mmol g<sup>-1</sup>).<sup>40</sup> Moreover, these values are higher than some materials with high surface areas such as COF-102 (3620 m<sup>2</sup> g<sup>-1</sup>, 1.52 mmol g<sup>-1</sup> at 273K and 1 bar),<sup>41</sup> and PAF-1 (5640 m<sup>2</sup> g<sup>-1</sup>, 2.07 mmol g<sup>-1</sup> at 273K and 1 bar).<sup>17</sup> Furthermore, the CO<sub>2</sub> uptake of N-H-1 outperforms the commercially available BPL carbon (2.09 mmol g<sup>-1</sup>).<sup>42</sup> Moreover, N-H-1 exhibits not only the highest gas uptake capacity of these two porous networks, but also with a higher isosteric heat (Q<sub>st</sub>) of 25.49-21.28 KJ mol<sup>-1</sup> (Fig. S8, ESI<sup>†</sup>). Based on the hydrogen sorption isotherms, we found that all isotherms were fully reversible and unsaturated at low pressures, and the hydrogen uptake capacities reached up to 0.92 wt% and 0.55 wt% for N-H-1 and N-H-2, respectively (Fig. 3(c)).

In summary, we report a new kind of fullerene-based porous materials with abundant pore structure and good gas adsorption properties, which employs the fullerene derivatives as building blocks to construct two different porous networks (N-H-1 and N-H-2) by using a novel and relatively low-cost strategy. The pore characteristics of these porous networks were calculated by surface area and porosity analyzer. The resulting products show good absorption properties for CO<sub>2</sub> and H<sub>2</sub>, thus making them promising candidates for applications

in gas adsorption. By using the novel synthetic strategy, fullerene-based HCPs materials can be constructed using relatively mild conditions, which makes the synthetic simple and more robust.

We thank the Analysis and Testing Centre, Huazhong University of Science and Technology for assistance in characterization of materials. This work was supported by the Program for National Natural Science Foundation of China (no.21474033), the International S&T Cooperation Program of China (2016YFE0124400), and the Program for HUST Interdisciplinary Innovation Team (2016JCTD104).

### Conflicts of interest

There are no conflicts to declare.

### Notes and references

1. Y. L. Luo, B. Y. Li, W. Wang, K. B. Wu and B. Tan, *Adv. Mater.*, 2012, **24**, 5703-5707.
2. J. H. Kou and L. B. Sun, *J. Mater. Chem. A*, 2016, **4**, 17299-17307.
3. L. B. Sun, Y. H. Kang, Y. Q. Shi, Y. Jiang and X. Q. Liu, *ACS Sustainable Chem. Eng.*, 2015, **3**, 3077-3085.
4. S. J. Xu, K. P. Song, T. Li and B. Tan, *J. Mater. Chem. A*, 2015, **3**, 1272-1278.
5. K. P. Song, Z. J. Zou, D. L. Wang, B. E. Tan, J. Y. Wang, J. Chen and T. Li, *J. Phys. Chem. C*, 2016, **120**, 2187-2197.
6. G. Das, B. P. Biswal, S. Kandambeth, V. Venkatesh, G. Kaur, M. Addicoat, T. Heine, S. Verma and R. Banerjee, *Chem. Sci.*, 2015, **6**, 3931-3939.
7. F. Beguin, V. Presser, A. Balducci and E. Frackowiak, *Adv. Mater.*, 2014, **26**, 2219-2251.
8. A. G. Slater and A. I. Cooper, *Science*, 2015, **348**, aaa8075.
9. S. Das, P. Heasman, T. Ben and S. Qiu, *Chem. Rev.*, 2017, **117**, 1515-1563.
10. J. X. Jiang, F. Su, A. Trewin, C. D. Wood, N. L. Campbell, H. Niu, C. Dickinson, A. Y. Ganin, M. J. Rosseinsky, Y. Z. Khimiyak and A. I. Cooper, *Angew. Chem., Int. Ed.*, 2007, **46**, 8574-8578.
11. X. S. Ding and B. H. Han, *Angew. Chem., Int. Ed.*, 2015, **54**, 6536-6539.
12. P. M. Budd, E. S. Elabas, B. S. Ghanem, S. Makhseed, N. B. McKeown, K. J. Msayib, C. E. Tattershall and D. Wang, *Adv. Mater.*, 2004, **16**, 456-459.
13. A. P. Cote, A. I. Benin, N. W. Ockwig, M. O'Keeffe, A. J. Matzger and O. M. Yaghi, *Science*, 2005, **310**, 1166-1170.
14. H. M. El-Kaderi, J. R. Hunt, J. L. Mendoza-Cortes, A. P. Cote, R. E. Taylor, M. O'Keeffe and O. M. Yaghi, *Science*, 2007, **316**, 268-272.
15. M. P. Tsyurupa and V. A. Davankov, *React. Funct. Polym.*, 2002, **53**, 193-203.
16. B. Y. Li, R. N. Gong, Y. L. Luo and B. E. Tan, *Soft Matter*, 2011, **7**, 10910-10916.
17. T. Ben, H. Ren, S. Ma, D. Cao, J. Lan, X. Jing, W. Wang, J. Xu, F. Deng, J. M. Simmons, S. Qiu and G. Zhu, *Angew. Chem., Int. Ed.*, 2009, **48**, 9457-9460.
18. Y. H. Xu, S. B. Jin, H. Xu, A. Nagai and D. L. Jiang, *Chem. Soc. Rev.*, 2013, **42**, 8012-8031.
19. H. W. Kroto, J. R. Heath, S. C. O'Brien, R. F. Curl and R. E. Smalley, *Nature*, 1985, **318**, 162-163.
20. T. T. Cao, N. Chen, G. X. Liu, Y. B. Wan, D. D. Perera, Y. C. Xia, Z. W. Wang, B. Song, N. Li, X. H. Li, Y. Zhou, C. J. Brabec and Y. F. Li, *J. Mater. Chem. A*, 2017, **5**, 10206-10219.
21. M. H. Stewart, A. L. Huston, A. M. Scott, E. Oh, W. R. Algar, J. R. Deschamps, K. Susumu, V. Jain, D. E. Prasuhn, J. Blanco-Canosa, P. E. Dawson and I. L. Medintz, *Acs Nano*, 2013, **7**, 9489-9505.
22. E. J. E. Stuart, K. Tschulik, C. Batchelor-McAuley and R. G. Compton, *Acs Nano*, 2014, **8**, 7648-7654.
23. J. Marco-Martinez, S. Reboredo, M. Izquierdo, V. Marcos, J. L. Lopez, S. Filippone and N. Martin, *J. Am. Chem. Soc.*, 2014, **136**, 2897-2904.
24. Z. Chen, L. Ma, Y. Liu and C. Chen, *Theranostics*, 2012, **2**, 238-250.
25. M. A. Lebedeva, T. W. Chamberlain and A. N. Khobystov, *Chem. Rev.*, 2015, **115**, 11301-11351.
26. L. Chen, K. Furukawa, J. Gao, A. Nagai, T. Nakamura, Y. P. Dong and D. L. Jiang, *J. Am. Chem. Soc.*, 2014, **136**, 9806-9809.
27. Y. Yuan, P. Cui, Y. Y. Tian, X. Q. Zou, Y. X. Zhou, F. X. Sun and G. S. Zhu, *Chem. Sci.*, 2016, **7**, 3751-3756.
28. S. Wang, C. Zhang, Y. Shu, S. Jiang, Q. Xia, L. Chen, S. Jin, I. Hussain, A. I. Cooper and B. Tan, *Sci. Adv.*, 2017, **3**, e1602610.
29. S. Wang, K. Song, C. Zhang, Y. Shu, T. Li and B. Tan, *J. Mater. Chem. A*, 2017, **5**, 1509-1515.
30. X. Y. Meng, W. Q. Zhang, Z. A. Tan, C. Du, C. H. Li, Z. S. Bo, Y. F. Li, X. L. Yang, M. M. Zhen, F. Jiang, J. P. Zheng, T. S. Wang, L. Jiang, C. Y. Shu and C. R. Wang, *Chem. Commun.*, 2012, **48**, 425-427.
31. J. Yang, L. B. Alemany, J. Driver, J. D. Hartgerink and A. R. Barron, *Chem. Eur. J.*, 2007, **13**, 2530-2545.
32. C. A. Reed, K. C. Kim, R. D. Bolskar and L. J. Mueller, *Science*, 2000, **289**, 101-104.
33. B. Li, R. Gong, W. Wang, X. Huang, W. Zhang, H. Li, C. Hu and B. Tan, *Macromolecules*, 2011, **44**, 2410-2414.
34. K. S. W. Sing, D. H. Everett, R. A. W. Haul, L. Moscou, P. A. Pierotti, J. Rouquerol and T. Siemieniowska, *Pure. Appl. Chem.*, 1985, **57**, 603-619.
35. J. Rouquerol, D. Avnir, C. W. Fairbridge, D. H. Everett, J. M. Haynes, N. Pernicone, J. D. F. Ramsay, K. S. W. Sing and K. K. Unger, *Pure. Appl. Chem.*, 1994, **66**, 1739-1758.
36. K. Wang, H. Huang, D. Liu, C. Wang, J. Li and C. Zhong, *Environ. Sci. Technol.*, 2016, **50**, 4869-4876.
37. K. S. Song, D. Kim, K. Polychronopoulou and A. Coskun, *ACS Appl. Mater. Interfaces*, 2016, **8**, 26860-26867.
38. D. Wang, W. Yang, S. Feng and H. Liu, *Rsc Adv.*, 2016, **6**, 13749-13756.
39. S. L. Wang, L. X. Tan, C. X. Zhang, I. Hussain and B. E. Tan, *J. Mater. Chem. A*, 2015, **3**, 6542-6548.
40. Y. W. Yang, B. Tan and C. D. Wood, *J. Mater. Chem. A*, 2016, **4**, 15072-15080.
41. Y. F. Zeng, R. Q. Zou and Y. L. Zhao, *Adv. Mater.*, 2016, **28**, 2855-2873.
42. Y. L. Luo, S. C. Zhang, Y. X. Ma, W. Wang and B. Tan, *Polym. Chem.*, 2013, **4**, 1126-1131.